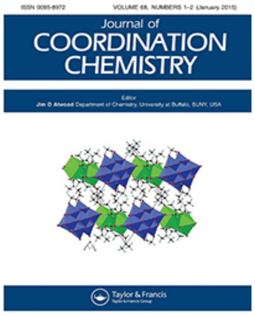

Taylor & Francis
Taylor & Francis Group

Journal of Coordination Chemistry

ISSN: 0095-8972 (Print) 1029-0389 (Online) Journal homepage: http://www.tandfonline.com/loi/gcoo20

Syntheses, structures, and fluorescent properties of four Co(II) coordination polymers based on 5-hydroxyisophthalic acid and structurally related bis(benzimidazole) ligands

Yong-Hong Wen, Run-Tao Dou, Kuo Yao & Guo-Feng Xu

To cite this article: Yong-Hong Wen, Run-Tao Dou, Kuo Yao & Guo-Feng Xu (2015) Syntheses, structures, and fluorescent properties of four Co(II) coordination polymers based on 5-hydroxyisophthalic acid and structurally related bis(benzimidazole) ligands, Journal of Coordination Chemistry, 68:1, 38-54, DOI: 10.1080/00958972.2014.983094

To link to this article: http://dx.doi.org/10.1080/00958972.2014.983094

Journal of Coordination Chemistry, 2015
Vol. 68, No. 1, 38–54, http://dx.doi.org/10.1080/00958972.2014.983094

Taylor & Francis
Taylor & Francis Group

Syntheses, structures, and fluorescent properties of four Co(II) coordination polymers based on 5-hydroxyisophthalic acid and structurally related bis(benzimidazole) ligands

YONG-HONG WEN*, RUN-TAO DOU, KUO YAO and GUO-FENG XU

Laboratory of Inorganic Synthesis and Applied Chemistry, College of Chemistry and Molecular Engineering, Qingdao University of Science and Technology, Qingdao, PR China

(*Received 9 March 2014; accepted 17 September 2014*)

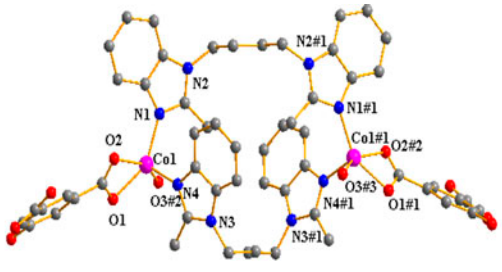

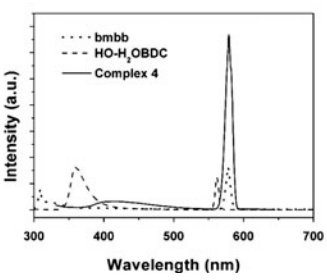

Four new cobalt(II) coordination polymers have been synthesized and characterized by elemental analyses, IR spectra, single crystal X-ray diffraction andthermogravimetric analyses. These four complexes all showed very strong yellowluminescence emission.

Four cobalt(II) coordination polymers, $\{[Co(HO\text{-}BDC)(bbp)]\}_n$ (**1**), $\{[Co(HO\text{-}BDC)(bmbp)_2]\cdot(H_2O)_2\}_n$ (**2**), $\{[Co(HO\text{-}BDC)(bbb)]\}_n$ (**3**), and $\{[Co_2(HO\text{-}BDC)_2(bmbb)_2]\cdot(H_2O)_3\}_n$ (**4**), where HO-H$_2$BDC = 5-hydroxyisophthalic acid, bbp = 1,3-bis(benzimidazol-1-yl)propane, bmbp = 1,3-bis(2-methyl-benzimidazol-1-yl)propane, bbb = 1,4-bis(benzimidazol-1-yl)butane, and bmbb = 1,4-bis(2-methyl-benzimidazol-1-yl)butane, have been synthesized and characterized by elemental analyses, IR spectra, single-crystal X-ray diffraction, thermogravimetric analyses, and fluorescence properties. Compounds **1** and **3** are 4-connected 2-D networks with $(4^4\cdot6^2)$ topology. Compound **2** is a 1-D chain, while **4** features a 1-D ladder. These 1-D and 2-D complexes are further connected by hydrogen bonds to form 3-D supramolecular architectures. Complexes **1–4** showed very strong yellow luminescence emission.

Keywords: Cobalt; Coordination polymer; Crystal structure; Fluorescence

---

*Corresponding author. Email: yonghwen@163.com

1. Introduction

There is interest in design and preparation of metal–organic coordination polymers, with intriguing structures and potential applications in luminescent materials, catalysis, magnetism, gas absorption, etc. [1–7]. A number of coordination polymers with promising properties have been synthesized by selection of metal centers with well-defined geometries, and organic linkers with suitable functionality and flexibility [8–12]. Particular attention has been devoted to coordination polymers constructed from aromatic polycarboxylic acids and bis(nitrogen-containing heterocycles) as mixed building blocks [13–16]. These ligands were chosen for the following reasons: (i) organic polycarboxylic acids possess a variety of coordination modes, and the acids can be both H-bond acceptors and donors to assemble supramolecular structures [17–21]; (ii) flexible bis(nitrogen-containing heterocycle) ligands often adopt different configurations to meet the coordination geometry requirements of metal ions and facilitate the formation of unusual coordination polymers [22, 23]; (iii) multi-dimensional supramolecular architectures can be fabricated easily from 1-D covalently bonded chains through hydrogen bond interactions in these mixed-ligand coordination polymers [24–27]; and (iv) combining different ligands in a complex offers greater tunability of structural frameworks than using single ligands, and the use of mixed-ligands is a good choice for construction of polymeric structures.

Mixed-ligand Co(II) coordination polymers with different structures and functions have been reported, most of which use pyridyl- or imidazole-containing ligands in metal-polycarboxylate systems [28–32]. However, studies on mixed-ligand Co(II) coordination polymers containing 5-hydroxyisophthalic acid (HO-H_2BDC) and bis(benzimidazole) ligands are less reported. We selected four bis(benzimidazole) compounds, 1,3-bis(benzimidazol-1-yl)propane (bbp), 1,3-bis(2-methyl-benzimidazol-1-yl)propane (bmbp), 1,4-bis(benzimidazol-1-yl) butane (bbb), and 1,4-bis(2-methyl-benzimidazol-1-yl)butane (bmbb), as auxiliary ligands (scheme 1) and synthesized four new cobalt(II) coordination polymers, $\{[Co(HO\text{-}BDC)(bbp)]\}_n$ (**1**), $\{[Co(HO\text{-}BDC)(bmbp)_2]\cdot(H_2O)_2\}_n$ (**2**), $\{[Co(HO\text{-}BDC)(bbb)]\}_n$ (**3**), and $\{[Co_2(HO\text{-}BDC)_2(bmbb)_2]\cdot(H_2O)_3\}_n$ (**4**). These compounds are characterized by elemental analyses, IR spectra, single-crystal X-ray diffraction, thermogravimetric analyses, and photoluminescent properties.

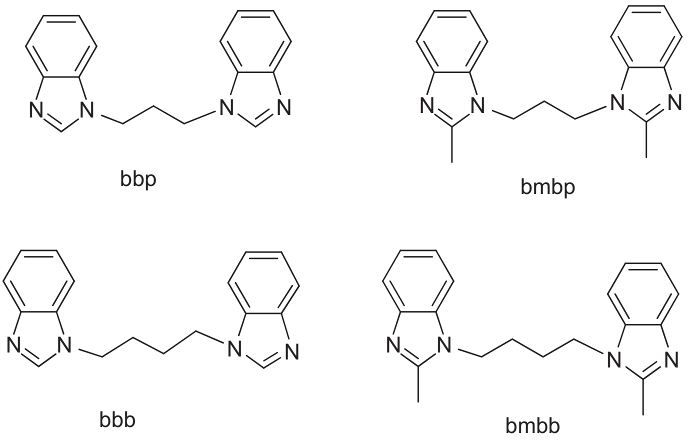

Scheme 1. Structures of bis(benzimidazole) ligands used in this work.

2. Experimental

2.1. *Materials and methods*

All commercially available reagents and chemicals were of analytical grade purity and used without purification. The four bisbenzimidazoles were prepared by the procedures reported [33–35]. The C, H, and N contents were determined using an Elementar Vario EL III analyzer. Infrared spectra were recorded from KBr pellets by a Nicolet 510P FT-IR spectrometer. Thermogravimetric analyses were performed on a Perkin–Elmer TG-7 analyzer heated from room temperature to 900 °C under an atmosphere of air, at a heating rate of 10 °C min^{-1}. Fluorescence measurements were made on a Hitachi F-4500 fluorescence spectrophotometer. The excitation spectra were obtained upon excitation at 340 nm for HO-H_2BDC, and at 375 nm for the four complexes as well as bis(benzimidazole) ligands.

2.2. *Synthesis of coordination polymers*

2.2.1. {[Co(HO-BDC)(bbp)]}$_n$ (1). A mixture of $CoCl_2·6H_2O$ (0.238 g, 1 mM), 1,3-bis(benzimidazol-1-yl)propane (0.276 g, 1 mM), 5-hydroxyisophthalic acid (0.365 g, 2 mM), NaOH (0.160 g, 4 mM), and 15 mL of H_2O was placed in a Parr Teflon-lined stainless steel vessel (25 mL). The vessel was sealed and heated to 140 °C for 72 h. Then the reactant mixture was cooled to room temperature, leading to formation of pink crystals of **1**. Yield 58% (based on $CoCl_2·6H_2O$). Anal. Calcd for $C_{25}H_{20}N_4O_5Co$ (%): C, 58.26; H, 3.91; N, 10.87. Found: C, 58.36; H, 3.83; N, 10.80. IR (KBr, cm^{-1}): 3420 (w), 3272 (w), 3118 (w), 3066 (w), 2945 (m), 1628 (m), 1587 (m), 1556 (s), 1510 (m), 1482 (w), 1464 (m), 1424 (m), 1390 (s), 1295 (w), 1274 (m), 1228 (w), 1200 (w), 1100 (w), 999 (w), 981 (w), 912 (w), 891 (w), 785 (m), 751 (m), 716 (m), 675 (w), 626 (w), 567 (w), 511 (w), 423 (w).

2.2.2. {[Co(HO-BDC)(bmbp)$_2$]·(H_2O)$_2$}$_n$ (2). A mixture of $CoCl_2·6H_2O$ (0.240 g, 1 mM), 1,3-bis(2-methyl-benzimidazol-1-yl)propane (0.304 g, 1 mM), 5-hydroxyisophthalic acid (0.365 g, 2 mM), NaOH (0.160 g, 4 mM), and 15 mL of H_2O was placed in a Parr Teflon-lined stainless steel vessel (25 mL). The vessel was sealed and heated to 140 °C for 72 h. Then the reactant mixture was cooled to room temperature, leading to formation of pink crystals of **2**. Yield 56% (based on $CoCl_2·6H_2O$). Anal. Calcd for $C_{46}H_{48}N_8O_7Co$ (%): C, 62.51; H, 5.47; N, 12.68. Found: C, 62.51; H, 5.47; N, 12.68. IR (KBr, cm^{-1}): 3397 (m), 3062 (w), 2960 (w), 2856 (w), 2715 (w), 1615 (m), 1581 (s), 1514 (m), 1476 (m), 1461 (s), 1444 (m), 1410 (s), 1381 (s), 1353 (s), 1291 (m), 1242 (w), 1160 (w), 1120 (w), 1100 (w), 1003 (w), 973 (w), 930 (w), 880 (w), 851 (w), 804 (w), 783 (m), 750 (m), 664 (w), 579 (w), 456 (w), 433 (w).

2.2.3. {[Co(HO-BDC)(bbb)]}$_n$ (3). A mixture of $CoCl_2·6H_2O$ (0.240 g, 1 mM), 1,4-bis(benzimidazol-1-yl)butane (0.290 g, 1 mM), 5-hydroxyisophthalic acid (0.365 g, 2 mM), NaOH (0.160 g, 4 mM), and 15 mL of H_2O was placed in a Parr Teflon-lined stainless steel vessel (25 mL). The vessel was sealed and heated to 140 °C for 72 h. Then the reactant mixture was cooled to room temperature, leading to formation of pink crystals of **3**. Yield 72% (based on $CoCl_2·6H_2O$). Anal. Calcd for $C_{26}H_{22}N_4O_5Co$ (%): C, 58.99; H, 4.19; N, 10.58.

Found: C, 58.99; H, 4.19; Co, 11.13; N, 10.58. IR (KBr, cm^{-1}): 3440 (m), 3116 (w), 3057 (w), 2947 (w), 2854 (w), 1637 (s), 1616 (w), 1556 (s), 1513 (m), 1481 (w), 1464 (m), 1443 (m), 1411 (s), 1390 (s), 1362 (m), 1335 (m), 1293 (w), 1278 (w), 1258 (w), 1225 (w), 1206 (w), 1195 (w), 1171 (w), 1119 (w), 1108 (w), 1010 (w), 1000 (w), 971 (w), 935 (w), 918 (w), 902 (w), 783 (m), 749 (s), 727 (m), 669 (w), 635 (w), 578 (w), 528 (w), 501 (w), 430 (w).

2.2.4. $\{[Co_2(HO\text{-}BDC)_2(bmbb)_2]\cdot(H_2O)_3\}_n$ (4). A mixture of $Co(NO_3)_2\cdot6H_2O$ (0.145 g, 0.5 mM), 1,4-bis(2-methyl-benzimidazol-1-yl)butane (0.159 g, 0.5 mM), 5-hydroxyisophthalic acid (0.091 g, 0.5 mM), NaOH (0.040 g, 1.0 mM), and 10 mL of H_2O was placed in a Parr Teflon-lined stainless steel vessel (25 mL). The vessel was sealed and heated to 160 °C for 72 h. Then the reactant mixture was cooled to room temperature, leading to formation of pink crystals of **4**. Yield 63% (based on $Co(NO_3)_2\cdot6H_2O$). Anal. Calcd for $C_{56}H_{58}N_8O_{13}Co_2$ (%): C, 57.54; H, 5.00; N, 9.59. Found: C, 57.66; H, 5.09; N, 9.49. IR (KBr, cm^{-1}): 3636 (m), 3427 (m), 3059 (m), 2944 (m), 1618 (m), 1577 (s), 1508 (m), 1479 (s), 1463 (s), 1411 (s), 1354 (s), 1290 (m), 1278 (m), 1237 (m), 1155 (m), 1012 (m), 792 (s), 784 (m), 748 (s), 719 (m), 656 (m), 622 (m), 466 (m), 436 (m).

2.3. *X-ray crystallography*

Single-crystal X-ray diffraction data of **1–4** were collected on a Bruker SMART 1000 CCD diffractometer with graphite monochromated Mo*Kα* radiation ($\lambda = 0.71073$ Å) using an ω scan mode, at room temperature. Intensity data were corrected for *Lp* factors and empirical absorption. The structures of **1–4** were solved by direct methods and expanded using Fourier differential techniques with SHELXTL [36]. All non-hydrogen atoms were located with successive difference Fourier syntheses. The structures were refined by full-matrix least-squares on F^2 with anisotropic thermal parameters for all non-hydrogen atoms. The hydrogens of phenol hydroxyl group in **1** and of water in **2** were located from the E-maps. The other hydrogens were geometrically fixed and allowed to ride on the parent atoms to which they are attached. In **3**, C8, C16, and C17 were disordered over two positions with occupancies of 0.50, respectively. The distribution of peaks in **4** was chemically featureless to refine using conventional discrete-atom models. So, the contribution of the electron density by the remaining water molecule was removed by the SQUEEZE routine in PLATON [37]. The number of solvent water molecules in **4** was determined by elemental analysis and thermogravimetric analysis. A summary of the key crystallographic data and structural refinements for **1–4** is presented in table 1. Selected bond distances and angles, and the hydrogen bond data for **1–4** are listed in tables 2 and 3.

3. Results and discussion

3.1. *Structure of $\{[Co(HO\text{-}BDC)(bbp)]\}_n$ (1)*

Single-crystal X-ray diffraction analysis reveals that **1** crystallizes in the orthorhombic crystal system of *Pbcm* space group in which the asymmetric unit contains half a Co(II), half a $HO\text{-}BDC^{2-}$, and half a bbp ligand. Co(II) is four-coordinate and resides in a slightly

Table 1. Crystal data and structure refinement information of **1–4**.

Compounds	**1**	**2**	**3**	**4**
Formula	$C_{25}H_{20}CoN_4O_5$	$C_{46}H_{48}CoN_8O_7$	$C_{26}H_{22}CoN_4O_5$	$C_{28}H_{26}CoN_4O_5$
Formula weight	515.38	883.85	529.41	557.46
Crystal system	Orthorhombic	Orthorhombic	Orthorhombic	Monoclinic
Space group	Pbcm	$Pca2_1$	Pnma	*I/2c*
a (Å)	9.463(7)	16.3440(4)	15.074(3)	18.2916(6)
b (Å)	14.588(3)	14.3295(5)	16.600(3)	20.5722(10)
c (Å)	16.064(5)	18.4308(5)	9.5296(18)	17.4711(7)
α (°)	90	90	90	90
β (°)	90	90	90	92.174(3)
γ (°)	90	90	90	90
V(Å^3)	2218(6)	4316.5(2)	2384.7(8)	6569.6(5)
Z	4	4	4	8
D (g cm^{-3})	1.544	1.360	1.475	1.127
μ (mm^{-1})	0.821	0.459	0.765	0.559
Crystal size (mm)	0.25 × 0.14 × 0.03	0.34 × 0.26 × 0.23	0.20 × 0.18 × 0.10	0.43 × 0.32 × 0.28
Total reflections	5776	14,109	11,106	16,447
Unique reflections	2256	6490	2176	6463
R (int)	0.0858	0.0535	0.0236	0.0490
R_1[a] (all data)	0.0830	0.0787	0.0510	0.1173
R_1[a] [$I > 2\sigma(I)$]	0.0526	0.0512	0.0417	0.0746
wR_2[b] (all data)	0.1488	0.1211	0.1170	0.2438
wR_2[b] [$I > 2\sigma(I)$]	0.1174	0.1000	0.1079	0.2140
GOF on F^2	1.049	1.027	1.027	1.121
Max/min.residual (e Å^{-3})	0.653/−0.638	0.497/−0.325	0.502/−0.404	0.540/−0.362

[a] $R = \sum \left| \, |F_o| - |F_c| \, \right| / \sum |F_o|$.

[b] $wR = [\sum w(F_o^2 - F_c^2)/\sum w(F_o^2)^2]^{1/2}$.

distorted tetrahedral coordination environment defined by two oxygens from two HO-BDC^{2-} ligands and two nitrogens from two bbp ligands (figure 1). All coordinated bond lengths (Co–O 1.936(4) and 1.951(4) Å, Co–N 2.040(4), and 2.040(4) Å) are in the normal range of other related complexes [38–43]. The angles around Co1 fall in the normal range of 103.4(2)–118.2(2)°. The two carboxylates of HO-BDC anion are unidentate (mode I, scheme 2). Each HO-BDC anion is a μ_2-bridge to connect metal ions to form a 1-D infinite chain in the a direction with Co–Co distances in the chain of 9.463 Å. Each bbp also is a μ_2-bridge linking metal ions to form a 1-D infinite chain in the c direction with Co–Co distance of 11.006 Å. A 2-D layer is constructed by coordination bonds and the 2-D layer structure shows a 4-connected network with ($4^4 \cdot 6^2$) topology (figure 2). The 2-D networks are further connected by O5–H5···O3 strong hydrogen bonds to form a 3-D architecture (figure 3). The distances of O5···O3 and the angles of O5–H5–O3 are 2.578(8) Å and 173 (9)°, respectively. The crystal structure is stabilized by π–π stacking interactions. The centroid–centroid distances between two imidazole rings (symmetry codes $-x + 1$, $-y + 1$, and $-z + 1$) are 3.817(7) Å and those between benzene and imidazole rings are 3.717(7) Å.

3.2. *Structure of {[Co(HO-BDC)(bmbp)$_2$]·(H$_2$O)$_2$}$_n$ (2)*

Compared with bbp, bmbp molecule adds a methyl in every benzimidazole ring, yet the complexes show completely different structures. Complex **2** crystallizes in the orthorhombic crystal system of $Pca2_1$ space group. The asymmetric unit contains one Co(II), one HO-BDC^{2-}, two bmbp ligands, and two lattice water molecules. The Co(II) is five-coordinate by two nitrogens from two bmbp and three oxygens from two carboxyl groups of two

Table 2. Selected bond lengths (Å) and angles (°) for **1–4**.

Complex **1**			
Co1–O1	1.936(4)	Co1–O4#2$^{\text{i}}$	1.951(4)
Co1–N1	2.040(4)	Co1–N1#3 $^{\text{ii}}$	2.040(4)
O1–Co1–O4#2$^{\text{i}}$	110.14(18)	O1–Co1–N1	103.44(11)
O4#2$^{\text{i}}$–Co1–N1#3$^{\text{ii}}$	110.48(11)	O1–Co1–N1#3 $^{\text{ii}}$	103.44(11)
O(4)#2–Co(1)–N(1)	110.48(11)	N1–Co1–N1#3$^{\text{ii}}$	118.2(2)
Symmetry codes: (i) $x-1, y, z$; (ii) $x, y, -z+1/2$; (iv) $x+1,y,z$.			
Complex **2**			
Co1–O3#1$^{\text{i}}$	1.983(3)	Co1–N5	2.065(4)
Co1–O1	2.064(3)	Co1–N1	2.077(4)
Co1–O2	2.261(3)		
O3 #1$^{\text{i}}$–Co1–O1	97.10(13)	N1–Co1–O2	88.07(15)
O3#1$^{\text{i}}$–Co1–N5	100.46(14)	O1–Co1–N5	113.44(15)
O3#1 $^{\text{i}}$–Co1–N1	104.45(14)	O1–Co1–N1	104.47(15)
N5–Co1–N1	131.07(15)	O3#1$^{\text{i}}$–Co1–O2	156.77(14)
O1–Co1–O2	60.42(12)	N5–Co1–O2	84.94(14)
Symmetry codes: (i) $x+1/2, -y+2, z$.			
Complex **3**			
Co1–O3#3$^{\text{i}}$	1.937(3)	Co1–O1	1.968(3)
Co1–N1	2.026(3)	Co1-N1#1$^{\text{ii}}$	2.026(3)
O3#3$^{\text{i}}$–Co1–O1	112.69(12)	O3#3$^{\text{i}}$–Co1–N1	103.70(9)
O1–Co1–N1	110.71(8)	O3#3$^{\text{i}}$–Co1–N1#1$^{\text{ii}}$	103.70(9)
O1–Co1–N1#1$^{\text{ii}}$	110.71(8)	N1–Co1–N1#1$^{\text{ii}}$	114.99(17)
Symmetry codes: (i) $x, y, z+1$; (ii) $x, -y+3/2, z$.			
Complex **4**			
Co1–O3#1$^{\text{i}}$	2.006(3)	Co1–N1	2.056(4)
Co1–O1	2.078(4)	Co1–N4	2.052(4)
Co1–O2	2.317(5)		
O3#1–Co1–N4	101.47(14)	N1–Co1–O1	147.70(19)
O(3)#1–Co1–N1	98.48(14)	O3#1–Co1–O2	152.95(18)
N4–Co1–N1	101.05(15)	N4–Co1–O2	93.99(18)
O3#1–Co1–O1	96.92(16)	N1–Co1–O2	100.18(15)
N4–Co1–O1	103.47(17)	O1–Co1–O2	57.59(18)
Symmetry codes: (i) $x-1/2, -y+3/2, z$.			

different HO-BDC^{2-} ligands, thus forming a distorted trigonal bipyramidal geometry (figure 4). O2 and O3#1 are located in axial positions with O2–Co1–O3#1 angles of 156.78(12)°, whereas the O1–Co1–N1, O1–Co1–N5, and N1–Co1–N5 angles around the metal center are 104.46(16), 113.46(15), and 131.07(16)°, respectively. All coordinated bond lengths (Co–O 1.983(3)–2.261(3) Å, Co–N 2.065(4)–2.077(4) Å) are in the normal range [38–43]. HO-BDC^{2-} adopts μ_2-bridging coordination to connect metal ions in a zigzag 1-D chain with Co–Co distances of 8.734 Å. One carboxylate is monodentate, while another chelates (mode II, scheme 2). Both bmbp ligands coordinate to metal ions monodentate. In **2**, the hydrogen bonds of two lattice water molecules play an important role in construction of the supramolecular structure. O7 is an acceptor forming a hydrogen bond with phenolic hydroxyl group (O5–H5···O7, N5···O7 2.632(6) Å, and O5–H5–O7 165.00°), and then O7 is a donor forming a hydrogen bond with O6 water (O7–H7B···O6, N7···O6 2.6031 Å, and O7–H7B–O6 164.00°). Meanwhile, O6 is an acceptor forming a hydrogen bond with carboxylate of the other HO-BDC^{2-} ligand (O6–H6B···O4, N6···O4 2.709(5) Å, and O6–H6B–O6 171.00°). These intermolecular hydrogen bonds connect 1-D chains to form a 2-D network (figure 5). Finally, O7 is again an acceptor forming a hydrogen bond with a N of bmbp (O7–H7A···N4, O7···N4 2.801(8) Å, and O7–H7A–N4 176.00°), while O6 is also a donor forming a

Table 3. Hydrogen bond data (Å) and (°) for **1–4**.

D–H···A	*d*(D–H)	*d*(H···A)	*d*(D···A)	∠DHA
Complex **1**				
O5–H5···O3[a]	0.82(8)	1.77(9)	2.578(8)	173(9)
C2–H2···O5[b]	0.93	2.44	3.324(9)	159
C4–H4···O4[a]	0.93	2.41	2.722(8)	100
C6–H6···O2	0.93	2.44	2.756(8)	100
C6–H6···O3	0.93	2.56	3.215(8)	128
C9–H9···O3[c]	0.93	2.52	3.192(7)	130
C11–H11···O1	0.93	2.51	3.197(8)	131
Symmetry codes: (a) 2 − *x*,−1/2 + *y*,1/2 − *z*; (b) 2 − *x*,1/2 + *y*,1/2−*z*; (c) −1 + *x*,*y*,*z*.				
Complex **2**				
O5–H5…O7a	0.82	1.83	2.632(6)	165
O6–H6A···N8b	0.85	2.02	2.817(8)	156
O6–H6B···O4c	0.85	1.86	2.709(5)	172
O7–H7A···N4d	0.85	1.95	2.801(8)	176
O7–H7B···O6	0.85	1.77	2.6031	164
C10–H10C···O3c	0.96	2.37	3.089(6)	131
C12–H12···O2	0.93	2.59	3.144(7)	118
C21–H21A···O2e	0.96	2.56	3.513(7)	170
Symmetry codes: (a) *x*,1 + *y*,*z*; (b) 1 − *x*,1 − *y*,1/2 + *z*; (c) 1/2 + *x*,2 − *y*,*z*; (d) 3/2 − *x*,−1 + *y*,−1/2 + *z*; (e) 1 − *x*,2 − *y*,1/2 + *z*.				
Complex **3**				
O5–H5A…O2a	0.73(6)	1.91(6)	2.636(4)	172(6)
C7–H7…O5b	0.96(5)	2.58(5)	3.505(5)	164(4)
C9–H9…O2	0.93(5)	2.44(5)	3.117(5)	130(4)
Symmetry codes: (a) 1/2 + *x*,3/2 − *y*,1/2-*z*; (b) −1/2 + *x*,3/2 − *y*,1/2 − *z*.				
Complex **4**				
O5–H5O4	0.82	1.95	2.770(5)	176
C9–H9B···O3	0.96	2.47	3.218(7)	135
C12–H12···O2	0.93	2.58	3.249(6)	129
C28–H28A···O1	0.96	2.52	3.396(7)	152
Symmetry codes: (a) 2 − *x*,*y*,1/2 − *z*; (b) −1/2 + *x*,3/2 − *y*,*z*.				

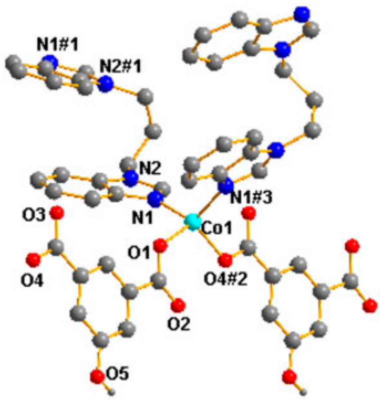

Figure 1. The coordination environment of **1**. Hydrogens except in phenol OH are omitted for clarity. Symmetry codes: #1 = *x*, −*y* + 3/2, −*z* + 1; #2 = *x* − 1, *y*, *z*; #3 = *x*, *y*, −*z* + 1/2.

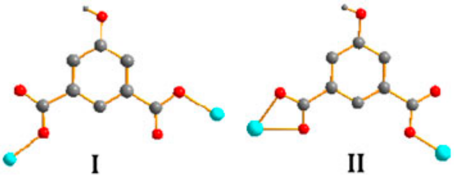

Scheme 2. Coordination modes of HO-H_2BDC in **1–4**.

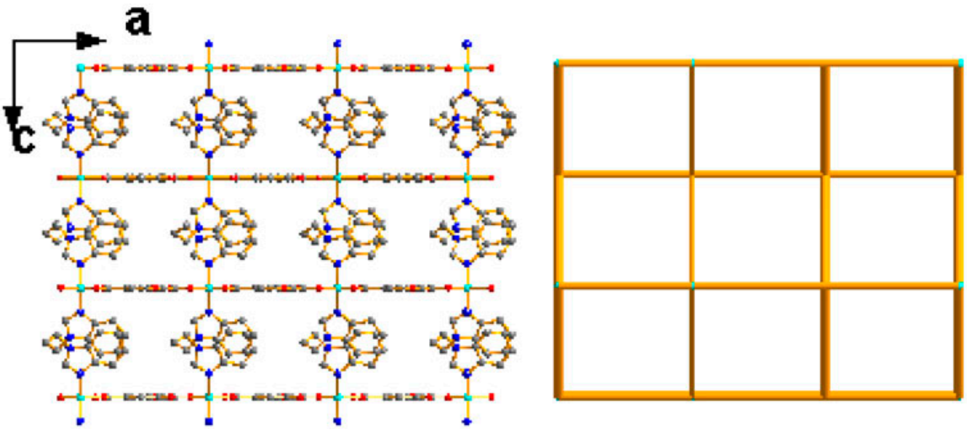

Figure 2. The 2-D layer structure of **1** (left) and schematic representation of the 4-connected network of **1** with ($4^4 \cdot 6^2$) topology (right).

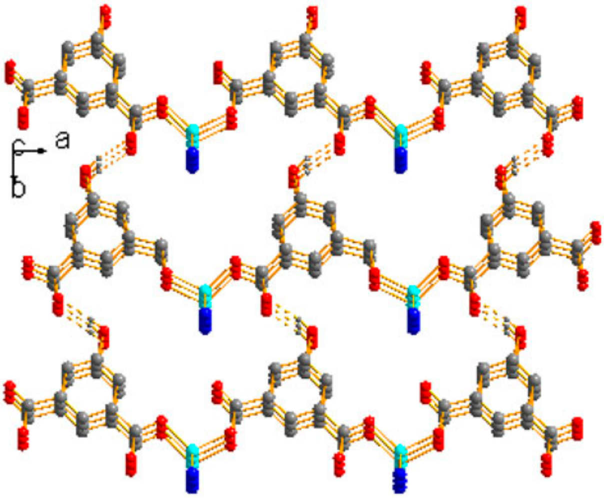

Figure 3. Hydrogen bond interactions between 2-D layers connecting **1** into a 3-D structure. Hydrogen bonds are shown in dash lines and bbp molecules are omitted for clarity.

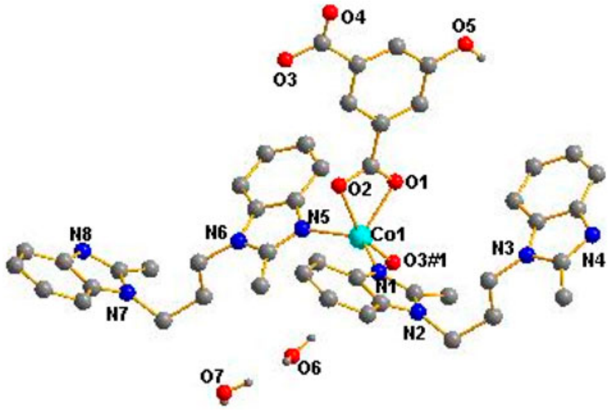

Figure 4. The molecular structure and coordination environment of **2**. Hydrogens except in phenol OH and water are omitted for clarity. Symmetry codes: #1 = *x* + 1/2, −*y* + 2, *z*.

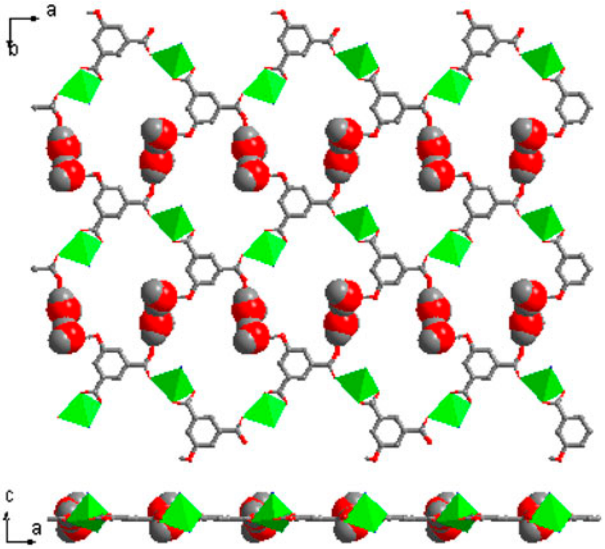

Figure 5. 2-D network of **2** formed by hydrogen bonds viewing along *c* (up) and *b* (down) axis. Cobalts are shown in polyhedra, hydrogen bonding water molecules in space-filling modes, and bmbp omitted for clarity.

hydrogen bond with a N of another bmbp (O6–H6A···N8, O6···N8 2.817(8) Å, and O6–H6A–N8 156.00°), thus finishing a 3-D supramolecular structure (figure 6).

3.3. *Structure of {[Co(HO-BDC)(bbb)]}$_n$ (3)*

Compared with bbp, bbb adds a methylene in the alkyl chain. Complex **3** crystallizes in the orthorhombic crystal system of *Pnma* space group in which the asymmetric unit contains

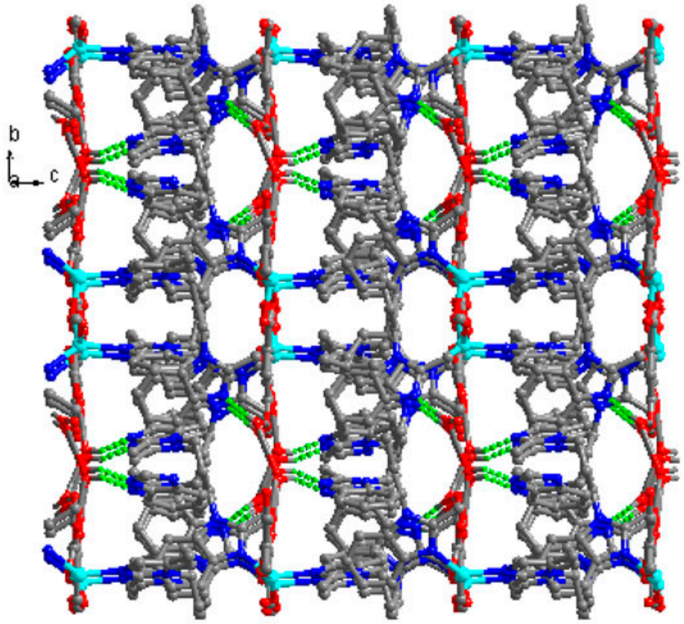

Figure 6. 3-D network of **2** formed by hydrogen bonds. Hydrogen bonds are shown as green dashed lines (see http://dx.doi.org/10.1080/00958972.2014.983094 for color version).

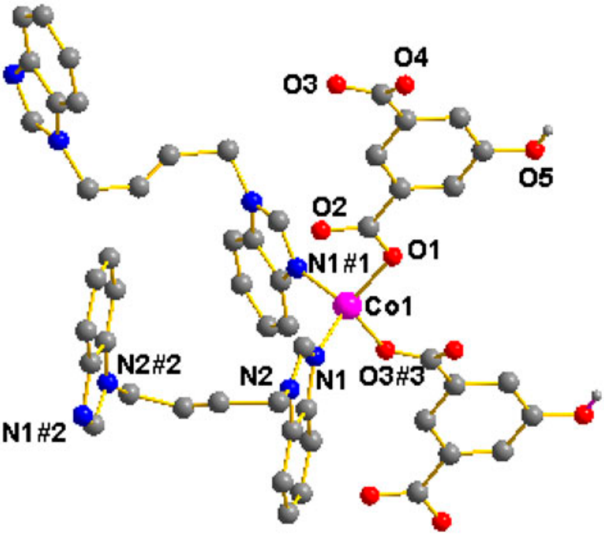

Figure 7. The coordination environment of **3**. Hydrogens except in phenol OH are omitted for clarity. Symmetry codes: #1 = x, $-y + 3/2$, z; #2 = $-x + 1$, $-y + 1$, $-z + 1$; #3 = x, y, $z + 1$.

half a Co(II), half a HO-BDC^{2-}, and half a bbb. Co(II) is four-coordinate by two oxygens from two HO-BDC^{2-} ligands and two nitrogens from two bbb ligands (figure 7). The coordination geometry of Co(II) is slightly distorted tetrahedral. All coordinated bond lengths

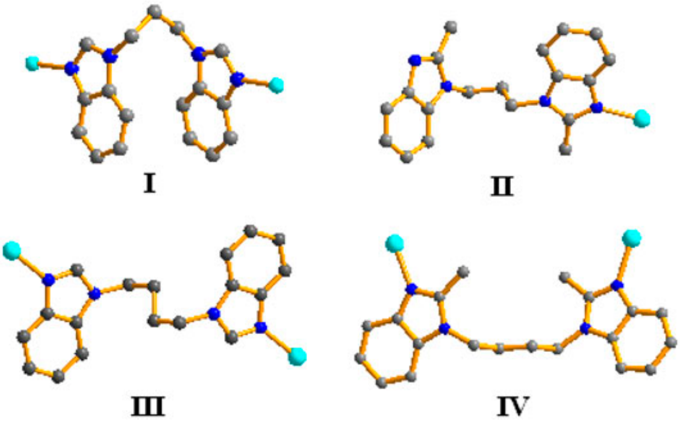

Scheme 3. Coordination modes of bisbenzimidazole ligands in **1–4**.

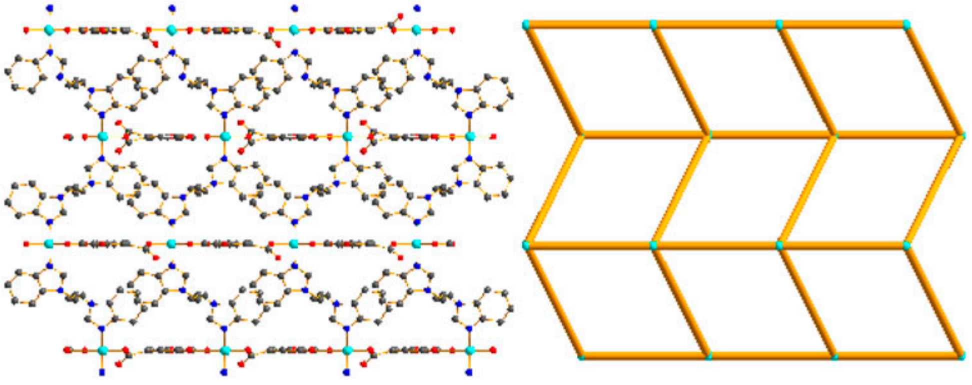

Figure 8. The 2-D layer structure of **3** (left) and schematic representation of the 4-connected network of **3** with $(4^4 \cdot 6^2)$ topology (right).

(Co–O 1.937(3) and 1.968(3) Å, Co–N 2.026(3), and 2.026(3) Å) are in the normal range, similar to values in related complexes [38–43]. The angles around Co1 fall in the normal range of 103.7(1) – 115.0(2)°. HO-BDC^{2-} adopts the same coordination as in **1** (mode I, scheme 2) and bridge metal ions to form 1-D infinite chains, which are connected by bbb to form a 2-D 4-connected network with $(4^4 \cdot 6^2)$ topology (figure 8). The 2-D networks are further connected by O5–H5A···O2 hydrogen bonds to form a 3-D supramolecular architecture. The distances of O5···O2 and the angles of O5–H5A–O2 are 2.634(4) Å and 172(6)°, respectively. In the 3-D framework, the Co–Co distances connected by HO-BDC^{2-}, by bbb, and by hydrogen bonds are 9.530, 12.519, and 7.561 Å, respectively.

3.4. *Structure of* $\{[Co_2(HO\text{-}BDC)_2(bmbb)_2]\}_n$ *(4)*

Compared with bbb, bmbb molecule adds a methyl in every imidazole ring. Complex **4** is a 1-D ladder, which crystallizes in the monoclinic crystal system of *I*/2*c* space group. As shown in figure 9, **4** consists of two Co(II) cations, two HO-BDC^{2-} anions, and two bmbb

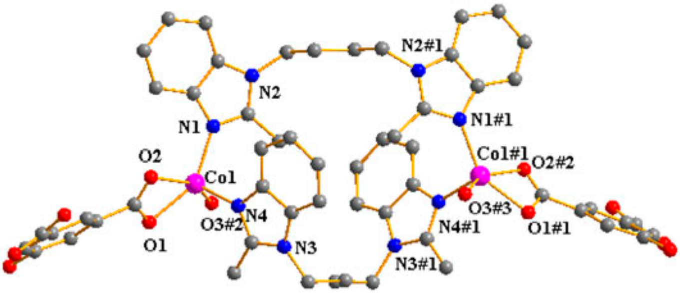

Figure 9. The molecular structure of **4**. Hydrogens are omitted for clarity. Symmetry codes: #1 = 1−*x*, *y*, −*z* + 3/2; #2 = *x*−1/2, −*y* + 3/2, *z*; #3 = −*x* + 3/2, −*y* + 3/2, −*z* + 3/2.

ligands. The asymmetric unit of **4** contains half the molecule, which is related to the other half by a crystallographic twofold axis. Co(II) is five-coordinate by three oxygens from two HO-BDC^{2-} ligands and two nitrogens from two bmbb ligands, exhibiting a square pyramidal geometry. All bond lengths (Co–O 2.006(3)–2.317(5) Å, Co–N 2.052(4)–2.056(4) Å) are comparable with those in related Co(II) complexes [38–43]. The HO-BDC^{2-} ligands have the same coordination as in **2** (mode II, scheme 2). In **4**, two bmbb ligands connect two central ions to form a dinuclear $Co_2(bmbb)_2$ unit, which is bridged by HO-BDC^{2-} anions to form a 1-D ladder (figure 10). In the 1-D ladder, the Co–Co distances connected by HO-BDC^{2-} and by bmbb are 9.307 and 9.821 Å, respectively. The 1-D ladders are connected by O5–H5···O4 hydrogen bonds into a 2-D net with the O5···O2 distance and the O5–H5A–O2 angle being 2.770(5) Å and 176°, respectively. Topologically, the two hydrogen-bond-connected HO-BDC^{2-} anions, (HO-BDC^{2-})$_2$, can be reduced to a 4-connected node, Co(II) can be considered as a 3-connected node, and bmbb ligands can be regarded as linkers between the Co(II) centers. Therefore, the framework of **4** can be described as a 3,4-connected network (figure 11).

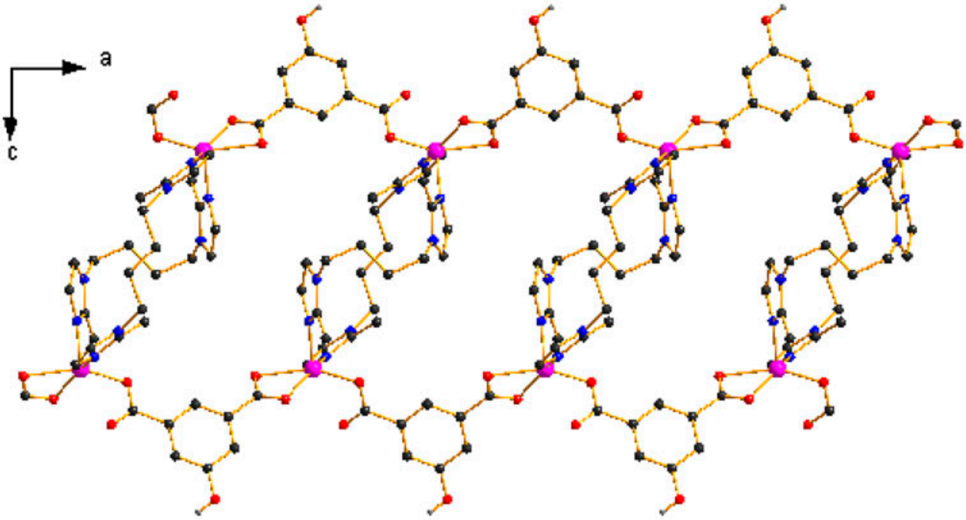

Figure 10. The 1-D ladder structure of **4** along the *a* axis. The benzene rings in benzimidazoles are omitted for clarity.

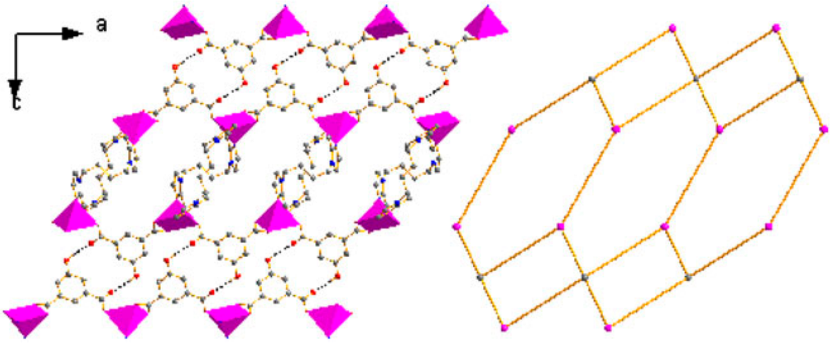

Figure 11. The 2-D layer structure of **4** (left) and schematic representation of the 3,4-connected network of **4** (right).

3.5. *Coordination modes of HO-H_2BDC in 1–4*

From the structure descriptions above, HO-H_2BDC can adopt two different coordination modes. In **1** and **3**, both two carboxylate groups of HO-BDC^{2-} ligand are $\mu_1{-}\eta^1:\eta^0$ (mode I, scheme 2). In **2** and **4**, one carboxylate of HO-BDC^{2-} is $\mu_1{-}\eta^0:\eta^1$ and the other $\mu_1{-}\eta^1:\eta^1$ (mode II, scheme 2).

3.6. *Effects of the N-donor ligands on the structures of 1–4*

The N-donor ligands have a significant effect on the structures. Among four N-donor ligands, bmbp is unidentate (mode II, scheme 3) while bbp, bbb, and bmbb exhibit bidentate/bridging coordination (modes I, III, and IV, scheme 3). In **1**, bbp is a μ_2-bridge to link two metal ions in the 1-D chain formed by HO-BDC^{2-} ligands and Co(II) ions to construct the 2-D layer. The 2-D layers are further connected by hydrogen bonds to form a 3-D architecture. In **2**, bmbp coordinates monodentate to metal ions in the 1-D chain. The 1-D chains are further linked by hydrogen bonds to form a 3-D supramolecular structure. In **3**, bbb bridges two Co centers in the 1-D chain formed by HO-BDC^{2-} ligands and Co(II) to form the 2-D 4-connected network, connected by hydrogen bonds to give the 3-D architecture. In **4**, bmbb bridges two metal ions to form the dinuclear $Co_2(bmbb)_2$ unit, bridged by HO-BDC^{2-} anions to form a 1-D ladder. The 1-D ladders are connected by hydrogen bonds into the 2-D 3,4-connected network. In **1**, **3,** and **4**, bidentate bbp, bbb, and bmbb exhibit different conformations. The bbp and bmbb show *cis*-conformation with dihedral angles between two benzimidazole rings of 10.23° and 18.7823°, respectively, while bbb displays *trans*-conformation with the dihedral angle between two benzimidazole rings of 0.00°. The different coordination modes of organic ligands lead to the different structures of **1–4**.

3.7. *Thermal analyses*

Thermogravimetric analyses were carried out for **1–4** to characterize the compounds more fully in terms of thermal stability. As shown in figure 12, **1** shows no weight loss from room temperature to 400 °C, but after this temperature, the compound decomposes rapidly. The weight loss corresponding to the decomposition of the organic components is observed from 400 to 520 °C (obsd 83.20%, calcd 83.90%). The remaining residue corresponding to

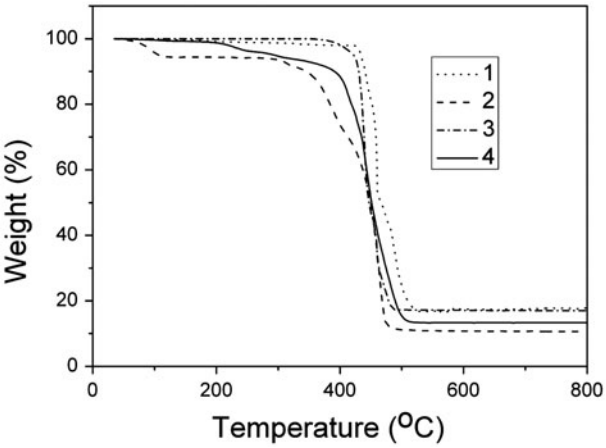

Figure 12. DTA curves of **1–4**.

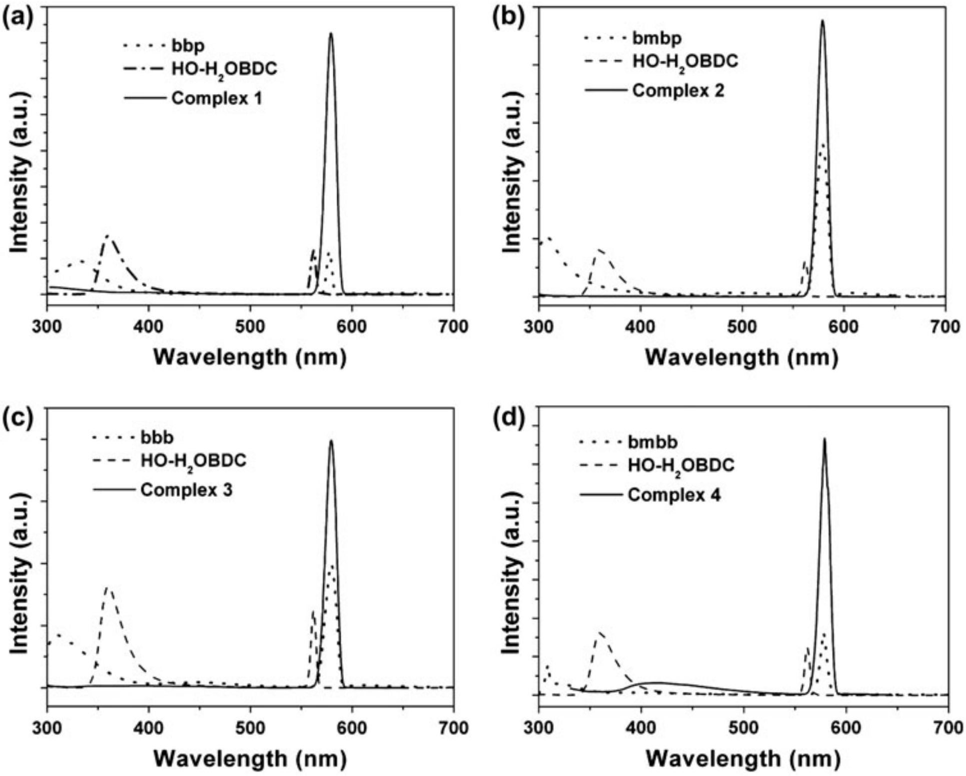

Figure 13. Solid state photoluminescent spectra of **1–4** (a–d) and related ligands.

the formation of Co_2O_3 is 17.64% (calcd 16.09%). Compound **2** shows a 4.19% weight loss from 30 to 100 °C, corresponding to loss of two lattice waters (calcd 4.08%). There is no weight loss from 100 to 300 °C. The second weight loss from 300 to 500 °C corresponds to decomposition of organic components (obsd 85.62%, calcd 86.54%). The remaining residue is 10.19%, corresponding to formation of Co_2O_3 (calcd 9.38%). For **3**, there is no weight loss from room temperature to 400 °C, and after this temperature, the compound decomposes rapidly. The weight loss corresponding to the decomposition is observed from 400 to 520 °C (obsd 83.20%, calcd 83.90%) and the remaining residue corresponding to formation of Co_2O_3 is 17.00% (calcd 16.09%). For **4**, the weight loss corresponding to release of the two lattice waters is observed from room temperature to 250 °C (obsd 4.10%, calcd 4.62%). The second weight loss from 260 to 550 °C corresponds to decomposition of organic components (obsd 82.70%, calcd 81.20%). The remaining residue is 13.20%, corresponding to formation of Co_2O_3 (calcd 14.18%).

3.8. *Photoluminescence properties*

The luminescence of the complexes, free HO-H_2BDC, and bis(benzimidazole) ligands were studied in the solid state at room temperature. As shown in figure 13, free HO-H_2BDC and four bis(benzimidazole) ligands all showed two weak to middle emissions with maximum wavelengths at 360 and 562 nm for HO-H_2BDC, 332 and 578 nm for bbp, 306 and 578 nm for bmbp, 310 and 575 nm for bbb, and 320 and 587 nm for bmbb, respectively. After coordination, the emission peaks of organic ligands at 310–360 nm disappeared, and only a strong emission at 579 nm for all four complexes was observed. This indicates that the coordination interactions between ligands and metal ions as well as ligand–ligand interactions such as π–π stacking and hydrogen bonding also play an important role in controlling the emission behavior of coordination polymers [44]. The strong luminescence emissions for these coordination polymers may be attributed to coordination of the ligands to metal ions, enhancing the conformational rigidity of the ligands, and thus decreasing the non-radiative energy loss [45, 46]. Generally speaking, Co(II) complexes emit weak photoluminescence at low temperature. Consequently, **1–4** are unusual examples of room temperature luminescent Co-containing polymers.

4. Conclusion

The reaction of four structurally related bis(benzimidazole) ligands with 5-hydroxyisophthalic acid and cobalt afforded four polymeric architectures. Two non-substituted bis-benzimidazole ligands, bbp and bbb, gave 2-D network structures, while two methyl-substituted bis-benzimidazole ligands, bmbp and bmbb, afforded 1-D coordination polymers, illustrating that the neutral bis-benzimidazole ligands play an important role in the construction of coordination polymers. The choice of N-donor compounds with different substituents and conformations as auxiliary ligands in the construction of coordination polymers can afford an opportunity to further enrich the structures and properties of coordination polymers. These compounds showed surprising thermal stability and very strong yellow luminescence emission. More mixed-ligand metal complexes based on N-containing ligands and polycarboxylate anions with interesting structures and properties will be prepared and applied as the solid materials.

Supplementary material

Crystallographic data for the structural analysis of the compounds has been deposited with the Cambridge Crystallographic Data Center. CCDC reference numbers 979657–979610 contain the supplementary crystallographic data for this paper. These data can be obtained free of charge from the Cambridge Crystallographic Data Center via www.ccdc.cam.ac.uk/data_request/cif.

Funding

This work was supported by the National Natural Science Foundation of China [grant number 20971076] and the Science and Technology Project of Shandong Province, China [grant number 2012G0020221].

References

[1] J.R. Li, R.J. Kuppler, H.C. Zhou. *Chem. Soc. Rev.*, **38**, 1477 (2009).
[2] O.K. Farha, C.D. Malliakas, M.G. Kanatzidis, J.T. Hupp. *J. Am. Chem. Soc.*, **132**, 950 (2009).
[3] L. Chen, G.J. Xu, K.Z. Shao, Y.H. Zhao, G.S. Yang, Y.Q. Lan, X.L. Wang, H.B. Xu, Z.M. Su. *CrystEngComm*, **12**, 2157 (2010).
[4] M. Ahmad, M.K. Sharma, R. Das, P. Poddar, P.K. Bharadwaj. *Cryst. Growth Des.*, **12**, 1571 (2012).
[5] M.D. Allendorf, C.A. Bauer, R.K. Bhakta, R.J.T. Houk. *Chem. Soc. Rev.*, **38**, 1330 (2009).
[6] Y. Gong, M.M. Zhang, W. Hua, J.L. Sun, H.F. Shi, P.G. Jiang, F.H. Liao, J.H. Lin. *Dalton Trans.*, **43**, 145 (2014).
[7] F. Meng, Z. Fang, Z. Li, W. Xu, M. Wang, Y. Liu, J. Zhang, W. Wang, D. Zhao, X. Guo. *J. Mater. Chem. A*, **1**, 7235 (2013).
[8] Z.G. Gu, X.X. Xu, W. Zhou, C.Y. Pang, F.F. Bao, Z.J. Li. *Chem. Commun.*, **48**, 3212 (2009).
[9] W.Q. Kan, J.F. Ma, B. Liu, J. Yang. *CrystEngComm*, **14**, 286 (2012).
[10] L. Qin, J.S. Hu, L.F. Huang, Y.Z. Li, Z.J. Guo, H.G. Zheng. *Cryst. Growth Des.*, **9**, 4176 (2010).
[11] L.L. Qu, Y.L. Zhu, J. Zhang, Y.Z. Li, H.B. Du, X.Z. You. *CrystEngComm*, **14**, 824 (2012).
[12] X.G. Guo, W.B. Yang, X.Y. Wu, Q.K. Zhang, L. Lin, R. Yu, H.F. Chen, C.Z. Lu. *Dalton Trans.*, **42**, 15106 (2013).
[13] J.S. Hu, Y.J. Shang, X.Q. Yao, L. Qin, Y.Z. Li, Z.J. Guo, H.G. Zheng, Z.L. Xue. *Cryst. Growth Des.*, **6**, 2676 (2010).
[14] W.Q. Kan, Y.Y. Liu, J. Yang, Y.Y. Liu, J.F. Ma. *CrystEngComm*, **13**, 4256 (2011).
[15] J. Chen, Y.L. Feng, Z.G. Jiang, J.W. Cheng. *CrystEngComm*, **13**, 6071 (2011).
[16] G.Y. Wang, L.L. Yang, Y. Li, H. Song, W.J. Ruan, Z. Chang, X.H. Bu. *Dalton Trans.*, **42**, 12865 (2013).
[17] C.H. Zhan, M.X. Jiang, Y.L. Feng, Y.H. He. *Polyhedron*, **29**, 2250 (2010).
[18] H. Abourahma, B. Moulton, V. Kravtsov, M.J. Zaworotko. *J. Am. Chem. Soc.*, **124**, 9990 (2002).
[19] Y.Y. Liu, J.F. Ma, J. Yang, Z.M. Su. *Inorg. Chem.*, **46**, 3027 (2007).
[20] A.J. Blake, N.J. Brooks, N.R. Champness, M. Crew, A. Deveson, D. Fenske, D.H. Gregory, L.R. Hanton, P. Hubberstey, M. Schroder. *Chem. Commun.*, **37**, 1432 (2001).
[21] Y.B. Go, X.Q. Wang, E.V. Anokhina, A.J. Jacobson. *Inorg. Chem.*, **43**, 5360 (2004).
[22] X.J. Li, X.Y. Wang, S. Gao, R. Cao. *Inorg. Chem.*, **45**, 1508 (2006).
[23] X.Y. Lan, S.L. Li, Y.M. Fu, Y.H. Xu, L. Li, Z.M. Su, Q. Fu. *Dalton Trans.*, **37**, 6796 (2008).
[24] Y. Yang, L.T. Yan, X.J. Luo, R.H. Qin, W.G. Duan. *Supramol. Chem.*, **24**, 810 (2012).
[25] H.Y. He, Y.L. Zhou, Y. Hong, L.G. Zhu. *J. Mol. Struct.*, **737**, 97 (2005).
[26] J.S. Lucas, L.D. Bell, C.M. Gandolfo, R.L. LaDuca. *Inorg. Chim. Acta.*, **378**, 269 (2011).
[27] L.F. Ma, L.Y. Wang, Y.W. Wang, J.L. Hu. *Cryst. Res. Technol.*, **9**, 995 (2008).
[28] A. Karmakar, H.M. Titi, I. Goldberg. *Cryst. Growth Des.*, **11**, 2621 (2011).
[29] J.Q. Liu, Y.Y. Wang, Y.S. Huang. *CrystEngComm*, **13**, 3733 (2011).
[30] A. Karmakar, I. Goldberg. *CrystEngComm*, **13**, 350 (2011).
[31] G.H. Wang, Y.Q. Lei, N. Wang, R.L. He, H.Q. Jia, N.H. Hu, J.W. Xu. *Cryst. Growth Des.*, **10**, 534 (2010).
[32] P. Lama, A. Aijaz, E.C. Sañudo, P.K. Bharadwaj. *Cryst. Growth Des.*, **10**, 283 (2010).
[33] Y. Wang, H.B. Xu, Z.M. Su, K.Z. Shao, Y.H. Zhao, H.P. Cui, Y.Q. Lan, X.R. Hao. *Inorg. Chem. Commun.*, **9**, 1207 (2006).
[34] Y.Y. Liu, J.F. Ma, J. Yang, J.C. Ma, Z.M. Su. *CrystEngComm*, **10**, 894 (2008).
[35] H.Y. Liu, H. Wu, J. Wang, Y.Y. Liu, B. Liu, Y.Y. Liu, J.F. Ma. *Cryst. Growth Des.*, **11**, 2920 (2011).
[36] G.M. Sheldrick. *Acta Crystallogr. A*, **64**, 112 (2008).

[37] A.L. Spek (Platon Program). *Acta Crystallogr. A*, **46**, 194 (1990).
[38] M.-L. Liu, Y.-X. Wang, W. Shi, J.-Z. Cui. *J. Coord. Chem.*, **65**, 1915 (2012).
[39] P.-F. Yao, C.-J. Ye, F.-P. Huang, H.-D. Bian, Q. Yu, K. Hu. *J. Coord. Chem.*, **66**, 1591 (2013).
[40] H.-W. Kuai, X.-C. Cheng, X.-H. Zhu. *J. Coord. Chem.*, **66**, 1795 (2013).
[41] B.-F. Huang, H.-P. Xiao, H. Huang, X.-H. Li, J.-G. Wang, A. Morsali. *J. Coord. Chem.*, **66**, 904 (2013).
[42] J.-H. Zhou, Y. Wang, S.-N. Wang, T. Wang, Y.-C. Chen, G.-X. Liu. *J. Coord. Chem.*, **66**, 737 (2013).
[43] W. Zhang, L.-J. Hao. *J. Coord. Chem.*, **66**, 2110 (2013).
[44] M.D. Allendorf, C.A. Bauer, R.K. Bhakta, R.J.T. Houk. *Chem. Soc. Rev.*, **38**, 1330 (2009).
[45] S.L. Zheng, J.H. Yang, X.L. Yu, X.M. Chen, W.T. Wong. *Inorg. Chem.*, **43**, 830 (2004).
[46] B. Valeur. *Molecular Fluorescence: Principles and Applications*., Wiley-VCH, New York, NY (2001).